Atmos. Chem. Phys. Discuss., doi:10.5194/acp-2016-144, 2016
Manuscript under review for journal Atmos. Chem. Phys.
Published: 18 February 2016

Atmospheric Chemistry and Physics Discussions

New insights into the atmospheric mercury cycling in Central Antarctica and implications at a continental scale

Hélène Angot[1], Olivier Magand[2, 1], Detlev Helmig[3], Philippe Ricaud[4], Boris Quennehen[2, 1], Hubert Gallée[2, 1], Massimo Del Guasta[5], Francesca Sprovieri[6], Nicola Pirrone[7], Joël Savarino[2, 1], Aurélien Dommergue[1, 2]

[1]Univ. Grenoble Alpes, Laboratoire de Glaciologie et Géophysique de l'Environnement (LGGE), 38041 Grenoble, France.

[2]CNRS, Laboratoire de Glaciologie et Géophysique de l'Environnement (LGGE), 38041 Grenoble, France.

[3]Institute of Arctic and Alpine Research (INSTAAR), University of Colorado, Boulder, CO 80309-0450, USA.

[4]CNRM/GAME, Météo-France/CNRS, 42 avenue de Coriolis, 31057 Toulouse, France.

[5]CNR-Istituto Nazionale di Ottica, Largo E. Fermi 6, Firenze, 50125, Italy.

[6]CNR-Institute of Atmospheric Pollution Research, Division of Rende, Italy.

[7]CNR-Institute of Atmospheric Pollution Research, Montelibretti, Rome, Italy.

Correspondence to: A. Dommergue (aurelien.dommergue@ujf-grenoble.fr)

Abstract

Under the framework of the GMOS project (Global Mercury Observation System) atmospheric mercury monitoring has been implemented at Concordia Station on the high-altitude Antarctic plateau (75°06'S, 123°20'E, 3220 m above sea level). We report here the first year-round measurements of gaseous elemental mercury (Hg(0)) in the atmosphere and in snowpack interstitial air on the East Antarctic ice sheet. This unique dataset shows evidence of a continuous oxidation of atmospheric Hg(0) in summer (24-hour daylight) due to the high oxidative capacity of the Antarctic plateau atmosphere at this period of the year. Summertime Hg(0) concentrations exhibited a pronounced daily cycle in ambient air with maximal concentrations around midday. Photochemical reactions and chemical exchange at the air/snow interface were prominent, highlighting the role of the snowpack on the

Atmos. Chem. Phys. Discuss., doi:10.5194/acp-2016-144, 2016
Manuscript under review for journal Atmos. Chem. Phys.
Published: 18 February 2016

atmospheric mercury cycle. Our observations reveal a 20 to 30% decrease of atmospheric Hg(0) concentrations from May to mid-August (winter, 24-h darkness). This phenomenon has never been observed elsewhere and likely results from a gas-phase oxidation and/or heterogeneous reactions. We also reveal the occurrence of multi-day to weeklong atmospheric Hg(0) depletion events in summer, not associated with depletions of ozone, and likely due to a stagnation of air masses above the plateau triggering an accumulation of oxidants within the shallow boundary layer. Our observations suggest that the inland atmospheric reservoir is depleted in Hg(0) in summer. Due to katabatic winds flowing out from the Antarctic plateau down the steep vertical drops along the coast and according to observations at coastal Antarctic stations, the striking reactivity observed on the plateau most likely influences the cycle of atmospheric mercury at a continental scale.

1 Introduction

Mercury biomagnifies in its methylated form in aquatic food webs to elevated levels in freshwater and marine fish, causing adverse health effects to wildlife and humans (Mason et al., 2012). In 2013, the Minamata Convention (UNEP, 2013) was adopted and opened for signature to reduce the exposure of populations to this worldwide contamination. Gaseous elemental mercury (Hg(0)), the most abundant form of mercury in the atmosphere, is efficiently transported around the globe, and even remote areas receive significant inputs of anthropogenic mercury by long-range atmospheric transport, as recently reported in modeling and observational studies (Weiss-Penzias et al., 2007; Lin et al., 2010).

Hg(0) can be oxidized into highly reactive and water-soluble gaseous and/or particulate divalent species (Hg(II) and Hg(p), respectively) (Lin and Pehkonen, 1999) leading to the formation and subsequent rapid deposition of reactive mercury onto environmental surfaces (Hedgecock and Pirrone, 2004). Upon deposition mercury can be reemitted back to the atmosphere or may enter the food chain through the conversion of Hg(II) to its methylated form (Driscoll et al., 2013). Effects and toxicity of mercury depends on this complex cycle, which is still not fully understood, and are only indirectly related to regional and global emissions (Driscoll et al., 2013). A better understanding of atmospheric mercury chemistry will lead to improved global transport and deposition models and could help refine pollution-control strategies around the world.

Atmos. Chem. Phys. Discuss., doi:10.5194/acp-2016-144, 2016
Manuscript under review for journal Atmos. Chem. Phys.
Published: 18 February 2016

New oxidation pathways, discovered in 1995 in the Arctic (Schroeder et al., 1998) and highlighting the influence of halogen radicals on Hg(0) oxidation in spring, changed our understanding of the mercury cycle. While the Arctic has been extensively monitored, there is still much to be learned from the Antarctic continent where studies are scarce (Dommergue et al., 2010), especially on the high altitude plateau (see Fig. 1). The Antarctic plateau – ice-covered area of ~ 7 million km^2 – was first considered to be chemically-inactive and a giant cold trap (Eisele et al., 2008) for atmospheric species, including mercury. It turned out to be highly photochemically active (Davis et al., 2001; Grannas et al., 2007) during the sunlit period with oxidant concentrations approaching those of tropical or urban mid-latitude environments (Eisele et al., 2008; Kukui et al., 2014). Earlier studies (Brooks et al., 2008; Dommergue et al., 2012) – the only two mercury studies ever carried out on the high-altitude Antarctic plateau with modern instruments – also suggested, based on short-term observations (a few weeks) in summer, an intense reactivity of mercury on the plateau at the air/snow interface. In this context, and under the framework of the GMOS project (Global Mercury Observation System, www.gmos.eu), atmospheric mercury was continuously monitored at Concordia Station (see Fig. 1) since 2012 and, for the first time, Hg(0) has been monitored year-round in both the snow interstitial air and the overlying atmosphere in 2013. Given harsh weather conditions (see section 2.1), and technical and logistical limitations, presenting such a record is in itself an important achievement. The main objective of this study is to provide new insights into the year-round cycling of gaseous mercury on the Antarctic plateau.

2 Experimental Section

2.1 Sampling site

Year-round measurements of gaseous mercury were conducted in 2012 and 2013 at the French/Italian Concordia Station (75°06’S, 123°20’E, 3220 m above sea level), located on the Antarctic plateau, 1100 km away from the nearest coast of East Antarctica (see Fig. 1). Concordia Station is a regional topographic maximum on the plateau; the surface terrain slopes do not exceed 1% (Genthon et al., 2010). The air temperature ranges between -20 °C in summer and -70 °C in winter, with an annual mean value of -45 °C (Pietroni et al., 2012). There is permanent daylight in summer and permanent darkness in winter. Snow accumulation is ~ 10 cm/year (Genthon et al., 2013).

Atmos. Chem. Phys. Discuss., doi:10.5194/acp-2016-144, 2016
Manuscript under review for journal Atmos. Chem. Phys.
Published: 18 February 2016

2.2 Sampling instrumentation

Instrumentation was located in a below-surface shelter at the edge of the "clean area", 800 m away from the main camp and upwind with respect to the dominant wind direction (south west). In 2012, year-round measurements were performed in the atmospheric boundary layer at about 500 cm above the snow surface. In 2013, measurements were performed in both the atmosphere and in snowpack interstitial air for several trace gases including gaseous mercury and ozone (O_3). Sampling instrumentation included one 10 m meteorological tower for above-surface gradient sampling and two multi-inlet snow sampling manifolds ("snow towers") for measuring trace gases at various depths in interstitial air (Bocquet et al., 2007; Seok et al., 2009). The 10 m meteorological tower was installed ~ 15 m upwind of the underground instrument shelter. It accommodated three gas inlets at 1070 cm, 210 cm, and 25 cm above the snow surface (see Fig. 2a). Trace gas measurements were acquired on each snow tower at six height levels: 50 and 10 cm above the snow surface, and 10, 30, 50, and 70 cm below the snow surface (see Fig. 2b). Sampling lines were purged continuously at 5 L/min on the meteorological tower and intermittently at ~ 2-3 L/min on the snow towers. On each snow tower, inlets were fitted with a small glass fibre filter in PTFE housing (25 mm Acrodisc syringe filters, Pall Life Sciences, Ann Arbor, Michigan, USA) to prevent snow crystals from entering the PFA sampling lines. Sampling lines were inside insulation tubing and the temperature of the sampling lines was maintained at a level 5-10 °C warmer than the snowpack temperature with a heat trace to prevent water vapor from freezing and clogging the lines. An automatic sampling pattern was implemented: trace gases were collected sequentially from the uppermost inlets on the meteorological tower to deepest levels of the snow towers. Measurements were taken for 10 min from each inlet.

2.3 Gaseous mercury measurements

Measurements were performed using a Tekran 2537A analyzer (Tekran Inc., Toronto, Canada) based on the amalgamation of mercury onto a gold cartridge followed by thermal desorption and detection by an integrated cold vapor atomic fluorescence spectrometer (CVAFS) at 253.7 nm (Fitzgerald and Gill, 1979; Bloom and Fitzgerald, 1988). The presence of two gold cartridges allowed alternating sampling and desorption modes and thus a continuous analysis in the pre-filtered (0.45 µm PTFE filter) and unheated sample air stream. The sampling resolution was 5 min with a sampling flow rate of 0.8 L/min. Concentrations are expressed in nanograms per cubic meter at standard temperature and pressure (273.15 K,

Atmos. Chem. Phys. Discuss., doi:10.5194/acp-2016-144, 2016
Manuscript under review for journal Atmos. Chem. Phys.
Published: 18 February 2016

1013.25 hPa). Using both a 0.45 µm PTFE filter at the entrance inlet of the sample line, and an unheated ¼"PTFE sample line, we assume that only Hg(0) (vs. total gaseous mercury, defined as the sum of gaseous mercury species) was efficiently collected and subsequently analyzed in this study (Steffen et al., 2002; Temme et al., 2003; Steffen et al., 2008).

Quality assurance and quality control procedures

An automatic calibration step of the Tekran 2537A analyzer was carried out every 25 h with an internal mercury permeation source. External calibrations were performed twice a year by injecting manually saturated mercury vapor taken from a temperature-controlled vessel (Tekran 2505 mercury vapor calibration unit, Hamilton digital syringe). As described by Angot et al. (2014), fortnightly to monthly routine maintenance operations were performed. A software programme was developed at the LGGE (Laboratoire de Glaciologie et Géophysique de l'Environnement) in accordance with quality control practice in well-established North American networks (Steffen et al., 2012). Based on various flagging criteria (Munthe et al., 2011; D'Amore et al., 2015), it enabled rapid data processing in order to produce clean time series of Hg(0). The detection limit is estimated at 0.10 ng/m^3 (Tekran, 2011).

2.4 Surface snow sampling and analysis

Surface snow samples (first cm) were collected weekly from February 2013 to January 2014 using acid cleaned PTFE bottles and clean sampling procedures. Upon collection, samples were stored in the dark at -20 °C. Field blanks, carried out by opening and closing a bottle containing mercury-free water, were regularly conducted. Surface snow samples and field blanks were analyzed for total mercury using a Tekran Model 2600. Quality assurance and quality control included the analysis of analytical blanks, replicates, internal standards, and spiked materials. The limit of quantification – calculated as 10 times the standard deviation of a set of 3 analytical blanks – amounted to 0.3 ng/L with a relative accuracy of ± 8%.

2.5 Ancillary parameters

Ozone

Measurements were performed using a UV absorption monitor (Thermo Electron Corporation, Franklin, MA), model 49I in 2012 (Legrand et al., Submitted to ACP) and model 49C in 2013. The instruments were calibrated against the National Oceanic and Atmospheric Administration Global Monitoring Division, Boulder, Colorado, standard.

Atmos. Chem. Phys. Discuss., doi:10.5194/acp-2016-144, 2016
Manuscript under review for journal Atmos. Chem. Phys.
Published: 18 February 2016

Air mass back trajectories

Air mass back trajectories were computed using the Lagrangian model FLEXPART (Stohl et al., 1998; Stohl and Thomson, 1999; Stohl et al., 2005) run in the backward mode and driven by NCEP (National Center for Environmental Predictions) GFS (Global Forecast System) final meteorological fields. Simulations were done every day at 1200 UTC in 2012 and 2013. For each simulation, 20000 pseudo-particles were released by the model around the position of Concordia Station and tracked for 5 days in three layers of altitude (0-0.1, 0.1-4 and 4-10 km above ground level). Simulations at an altitude of 4-10 km were computed in order to investigate the potential occurrence of upper troposphere/lower stratosphere intrusions. For each 1-h time step, the model produced a normalized particle residence time (in seconds) within an output grid of 0.5x0.5°. The sum of the 5 days outputs provided potential emission sensitivities (PES, in seconds) for the three layers of altitude. PES in a particular grid cell is proportional to the particle residence time in that cell. It should be noted that, in Antarctica, the meteorological data driving the FLEXPART transport model rely on sparse measurements. Consequently, the trajectories calculated in this region are often associated with relatively high uncertainties.

Height of the boundary layer and shortwave radiation

The height of the boundary layer and downwelling shortwave radiation were calculated by the MAR regional atmospheric model (Modèle Atmosphérique Régional). MAR was developed at the LGGE for Polar Regions and the simulations have been evaluated against meteorological observations made at Concordia Station (Gallée and Gorodetskaya, 2010; Gallée et al., 2015).

Meteorological data

Temperature, wind speed and direction were recorded at six height levels on a 45 m tower. The general observation set up is described by Genthon et al. (2010).

Ice precipitation

A tropospheric depolarization LIDAR (Light Detection And Ranging) operating at 523 nm provided tropospheric profiles of aerosol and clouds every 5 min allowing detection of water/ice clouds, snow drift, diamond dust and pollution plumes.

Tropospheric temperature and integrated water vapor

Atmos. Chem. Phys. Discuss., doi:10.5194/acp-2016-144, 2016
Manuscript under review for journal Atmos. Chem. Phys.
Published: 18 February 2016

A H_2O Antarctica Microwave Stratospheric and Tropospheric Radiometers (HAMSTRAD) instrument was used for the detection of the 60-GHz oxygen and the 183-GHz water vapor lines allowing measurement of tropospheric temperature and water vapor profiles, respectively, together with integrated water vapor (IWV) every 7 min. The instrument is fully automated and a liquid nitrogen calibration is performed twice per year (Ricaud et al., 2015).

Eddy diffusivity and friction velocity

The Eddy diffusivity was calculated as follows (Xiao et al., 2014):

$$K = k\, u_* \, z/\varphi_h \qquad (1)$$

where k (set to 0.40) is the von Karman constant, u_* the friction velocity (m/s), z the measurement height (m), and φ_h the Obukhov stability function. According to Frey et al. (2013), the stability function was $\varphi_h = 0.95 + 4.62\frac{z}{L}$ for stable conditions above snow (King and Anderson, 1994), and $\varphi_h = 0.95\left(1 - 11.6\frac{z}{L}\right)^{-0.5}$ for unstable conditions (Hoegstroem, 1988). u_* and L (the Obukhov length (m)) were computed from the three-dimensional wind components (*u*, *v*, *w*) and temperature measured by a Metek sonic anemometer mounted at 8 m above the snow surface.

3 Results and Discussion

3.1 Seasonal variation of Hg(0) in ambient air

The seasonal boundaries were defined according to the transitions in downwelling shortwave radiation (see Fig. 3b) as follows: winter from May to mid-August, spring from mid-August to October, summer from November to mid-February, and fall from mid-February to April.

The record of atmospheric Hg(0) over the entire 2012-2013 period is displayed in Fig. 3a. Hg(0) concentrations ranged from below 0.10 to 2.30 ng/m^3, with average values amounting to 0.76 ± 0.24 ng/m^3 in 2012, and to 0.81 ± 0.28 ng/m^3, 0.84 ± 0.27 ng/m^3, and 0.82 ± 0.26 ng/m^3 in 2013 at 25, 210, and 1070 cm above the snow surface, respectively. No significant difference was observed between annual averages of Hg(0) concentrations measured at the three inlets of the meteorological tower in 2013 (p value = $3.1.10^{-14}$, Mann-Whitney test). These mean annual Hg(0) concentrations are lower than annual averages reported at coastal Antarctic stations (i.e., 0.93 ± 0.19 ng/m^3 for Hg(0) at Troll (Pfaffhuber et al., 2012) and 1.06 ± 0.24 ng/m^3 for total gaseous mercury at Neumayer (Ebinghaus et al., 2002)).

Atmos. Chem. Phys. Discuss., doi:10.5194/acp-2016-144, 2016
Manuscript under review for journal Atmos. Chem. Phys.
Published: 18 February 2016

Unlike in winter, Hg(0) concentrations were highly variable during the sunlit period with concentrations ranging from below 0.10 ng/m^3 to 1.50-2.00 ng/m^3, up to twice the average background levels recorded in the Southern Hemisphere mid-latitudes (Slemr et al., 2015). These seasonal features, in good agreement with observations at other Antarctic stations (Ebinghaus et al., 2002; Pfaffhuber et al., 2012), suggest the existence of a photochemically-induced reactivity of atmospheric mercury during the sunlit period.

3.2 Summertime continuous oxidation of Hg(0) in ambient air and Hg(II) deposition onto snowpack

In summer, the mean atmospheric Hg(0) concentration was 0.69 ± 0.35 ng/m^3. This means that Hg(0) concentrations are ~ 25% lower than levels recorded at the same period of the year at coastal Antarctic stations (Pfaffhuber et al., 2012; Ebinghaus et al., 2002; Sprovieri et al., 2002). Total mercury concentrations in surface snow samples were highly variable (median value: 4.8 ng/L, range: < detection limit – 73.8 ng/L, see Fig. 4) and were higher in summer (median value: 10.4 ng/L, range: 1.3 – 73.8 ng/L), suggesting that divalent mercury species were preferentially deposited onto the snowpack at this period of the year. The lower Hg(0) concentrations in ambient air along with high total mercury concentrations in surface snow samples suggest a continuous oxidation of Hg(0) in ambient air in summer, followed by the deposition of oxidation products on surface snow. This hypothesis is further supported by elevated oxidized mercury concentrations measured on the Antarctic plateau at South Pole in summer (0.10 – 1.00 ng/m^3) by Brooks et al. (2008).

The oxidative capacity of the Antarctic plateau atmosphere is elevated in summer, as evidenced by several studies (Davis et al., 2001; Grannas et al., 2007; Eisele et al., 2008; Kukui et al., 2014), likely explaining this continuous oxidation of Hg(0) in ambient air. Among these oxidants, NO_2, RO_2, and OH are particularly abundant at Concordia Station in summer (Frey et al., 2013; Kukui et al., 2014) and a recent study provided as a first estimate a BrO mixing ratio of 2-3 pptv near the ground during sunlight hours (Frey et al., 2015). Given the current understanding of mercury oxidation and the lack of continuous halogens measurements, we were not able to identify the exact mechanism for the reactivity observed at Concordia Station. A two-step oxidation mechanism, favored at cold temperatures, is worth being considered further. The initial recombination of Hg(0) and Br is followed by the addition of a second radical (e.g., I, Cl, BrO, ClO, OH, NO_2, or HO_2) in competition with thermal dissociation of the HgBr intermediate (Goodsite et al., 2004; Wang et al., 2014).

Atmos. Chem. Phys. Discuss., doi:10.5194/acp-2016-144, 2016
Manuscript under review for journal Atmos. Chem. Phys.
Published: 18 February 2016

According to Dibble et al. (2012), HO_2, NO, NO_2, and NO_3 bound Hg(0) too weakly to initiate its oxidation in the gas phase and reactions of the HgBr intermediate with NO_2, HO_2, ClO, and BrO are more important than with Br and OH. Further modeling or laboratory chamber studies investigating the fate of Hg(0) in the presence of various potential oxidants are needed to improve our understanding of the mechanisms.

3.3 Hg(0)/Hg(II) redox conversions within the snowpack

Hg(0) moves easily between the atmosphere and the cryosphere (Durnford and Dastoor, 2011). A fraction of deposited mercury species can be reduced (the reducible pool) and subsequently reemitted to the atmosphere as Hg(0). Reduced mercury can concurrently be reoxidized within the snowpack. In Fig. 5, the redox processes occurring within the snowpack are shown along with several other processes that govern mercury exchange at the air/snow interface. These processes are discussed in details in the following sections.

3.3.1 Sunlit period

Fig. 6 depicts the mean Hg(0) concentration at various heights above and below the snow surface (in the interstitial air of the snow) for all seasons. During the sunlit period (summer, spring/fall), Hg(0) concentration peaked in the upper layers of the snowpack and then decreased with depth, with levels in the snow interstitial air (SIA) dropping below atmospheric values.

Hg(0) is generally produced in the upper layers of the snowpack – as the result of a photolytically initiated reduction of Hg(II) (Lalonde et al., 2003) – and diffuses upward and downward. According to our observations, Hg(0) concentration peaked at ~ 10 cm below the snow surface (see Fig. 6). Similarly, Brooks et al. (2008) reported Hg(0) concentrations peaking at a depth of 3 cm at South Pole. Below the top layer, the actinic flux decreases exponentially with depth (King and Simpson, 2001; Domine et al., 2008). The light penetration depth (*e*-folding depth) is the depth at which the actinic flux's magnitude is 1/*e* of its incident value (Perovich, 2007). It is estimated that ~ 85% of the photoreduction occurs in the top two *e*-folding depths (King and Simpson, 2001). At Concordia Station, the *e*-folding depth is ~ 10 cm at 400 nm for the windpack layers (France et al., 2011), which supports our observations. As previously mentioned, reduced mercury can concurrently be reoxidized within the snowpack. Below the top layer, Hg(0) concentration in the SIA dropped with depth (see Fig. 6) suggesting that oxidation dominated in the deepest layers – in good agreement

Atmos. Chem. Phys. Discuss., doi:10.5194/acp-2016-144, 2016
Manuscript under review for journal Atmos. Chem. Phys.
Published: 18 February 2016

with observations within the snowpack at Kuujjuarapik/Whapmagoostui, Québec, Canada (Dommergue et al., 2003) – leading to the formation of a Hg(II) reservoir.

The amount of Hg(0) emitted from the snowpack to the atmosphere depends on the balance of reduction and oxidation processes within the upper layers of the snowpack (Durnford and Dastoor, 2011). Fig. 7 depicts the hourly mean atmospheric and interstitial air Hg(0) concentrations. Our observations indicate that summertime Hg(0) concentration in the upper layers of the snowpack exhibited a diurnal cycle and peaked in the afternoon (see Fig. 7a, lower panel). Conversely, in spring/fall, Hg(0) concentration reached a maximum at night and a minimum near midday in the upper layers of the snowpack (see Fig. 7b). The balance of reduction and oxidation processes within the upper layers of the snowpack suddenly shifted in summer. Similarly, Faïn et al. (2008) found that reduction dominated during summer and oxidation in spring in the upper layers of the snowpack at Summit, Greenland.

It is worth noting that Hg(0) concentration in the SIA was occasionally very high. For instance, on 24 February 2013, Hg(0) concentration reached 3.00 ng/m^3 at a depth of 10 cm. During this event, ice precipitation was observed at Concordia Station with depolarization values greater than 30% (see Fig. 8). This suggests that the presence of ice crystals could enhance the dry deposition of Hg(II) species onto the snow surface leading to increased Hg(0) formation in the upper layers of the snowpack. Indeed, due to an elevated specific surface area, mercury-capture efficiency of ice crystals is high (Douglas et al., 2008). Unfortunately, due to a low sampling frequency of surface snow samples (weekly), total mercury concentrations cannot be used to study further the relationship between the occurrence of ice precipitation events and dry deposition of mercury species.

3.3.2 Winter

Contrarily to the sunlit period, Hg(0) concentration increased with depth in the SIA in winter (see Fig. 6). The average (winter) Hg(0) concentration amounted to 3.60 ng/m^3 at a depth of 70 cm and was observed at a temperature of about -60 °C and not related to any change in atmospheric composition. Our observations are in agreement with earlier studies indicating that reduction of Hg(II) species is possible in the dark (Ferrari et al., 2004; Faïn et al., 2007; Ferrari et al., 2008). The production of Hg(0) might be due to the reduction of Hg(II) species accumulated in the deepest layers of the snowpack during the sunlit period (see section 3.3.1). This shift from oxidation to reduction in the deepest layers of the snowpack at the beginning of winter remains unexplained.

Atmos. Chem. Phys. Discuss., doi:10.5194/acp-2016-144, 2016
Manuscript under review for journal Atmos. Chem. Phys.
Published: 18 February 2016

3.4 Boundary layer dynamics and its influence on Hg(0) in ambient air

Several studies highlighted that the atmospheric turbulence at Concordia Station in summer influences the vertical flux and concentration profiles of various atmospheric species (Legrand et al., 2009; Dommergue et al., 2012; Kerbrat et al., 2012; Frey et al., 2013).

3.4.1 Summertime Hg(0) diurnal cycle

Based on a week of measurements made at Concordia Station in January 2009, Dommergue et al. (2012) reported that atmospheric Hg(0) exhibited a significant and daily cycle with maximal concentrations around noon. We show that this daily cycle occurred all along the summer, with low atmospheric Hg(0) concentrations (~ 0.50 ng/m^3) when solar radiation was minimum and a maximum (~ 0.80 ng/m^3) around noon (see Figs. 7a, upper panel and 9g). Such a pronounced daily cycle has never been observed at other Antarctic stations (Dommergue et al., 2010; Pfaffhuber et al., 2012). Several studies showed that Hg(0) emission from the snowpack maximizes near midday (e.g., Steffen et al., 2002; Ferrari et al., 2005; Brooks et al., 2006; Faïn et al., 2007; Ferrari et al., 2008; Johnson et al., 2008). As suggested by Durnford and Dastoor (2011), the noon emission does not necessarily reflect maximum concentrations of cryospheric Hg(0) around midday (Hg(0) concentration peaked in the afternoon at 10 cm below the snow surface, see section 3.3.1) and could be driven by ventilation generated by atmospheric thermal convection. Stable boundary layers are almost ubiquitous in Polar Regions due to radiation cooling (Anderson and Neff, 2008). However, convective boundary layers have been observed in summer at polar domes at Concordia Station (King et al., 2006) and Summit in Greenland (Cohen et al., 2007). Fig. 9 displays the hourly mean variation of several parameters. As illustrated by Figs. 9a and 9c, and in agreement with earlier observations (e.g., Argentini et al., 2005; Pietroni et al., 2012; Argentini et al., 2013), there was a strong diurnal cycle in near-surface temperature and wind speed in summer at Concordia Station. These observations are typical for locations where a convective boundary layer develops as a response to daytime heating (King et al., 2006), as can be seen in Fig. 9d. In a convective boundary layer, vertical mixing is enhanced during convective hours (Anderson and Neff, 2008), as shown in Figs. 9e and 9f by increasing values for the Eddy diffusivity (K) and the friction velocity (u_*, indicative of the strength of the mixing processes in the surface layer (Neff et al., 2008)).

In summary, the observed summertime Hg(0) diurnal cycle in ambient air might be due to a combination of factors: i) a continuous oxidation of Hg(0) in ambient air due to the high

Atmos. Chem. Phys. Discuss., doi:10.5194/acp-2016-144, 2016
Manuscript under review for journal Atmos. Chem. Phys.
Published: 18 February 2016

oxidative capacity on the plateau, ii) important Hg(II) deposition onto snowpack, and iii) important emission of Hg(0) from the snowpack during convective hours following photoreduction of Hg(II) in the upper layers of the snowpack.

3.4.2 Elevated Hg(0) concentrations in fall

In fall, Hg(0) concentrations in ambient air no longer peaked around midday (see Fig. 9g) and were in average 67% higher than during the summer, exceeding levels recorded at lower latitudes in the Southern Hemisphere (Slemr et al., 2015). At this period of the year, the boundary layer lowered to ~ 50 m in average and no longer exhibited a pronounced diurnal cycle (see Figs. 3c and 9d). We believe that the shallow boundary layer could cause Hg(0) concentrations in ambient air to build up to where they exceeded levels recorded at lower latitudes in the Southern Hemisphere because Hg(0) was dispersed into a reduced volume of air, limiting the dilution. Similarly, NOx mixing ratios are enhanced when the boundary layer is shallow (Neff et al., 2008; Frey et al., 2013). Elevated Hg(0) concentrations were also likely favored by the fact that oxidation in ambient air was weaker under lower solar radiation.

3.5 Multi-day depletion events of atmospheric Hg(0)

First discovered in the Arctic (Schroeder et al., 1998), atmospheric Hg(0) depletion events result from an oxidation by reactive bromine species released during springtime explosions in coastal regions (Durnford and Dastoor, 2011 and references therein) and are concurrent with tropospheric O_3 depletion events (Simpson et al., 2007). Despite the distance of Concordia Station from the coast (1100 km), a Hg(0) depletion event was observed on 11 September 2013 due to a maritime air transport event (see Fig. 10e). During this event, Hg(0) concentrations exhibited a strong positive correlation with O_3 mixing ratios (rho = 0.94, *p* value = 5.10^{-7}).

From 19 January to 8 February 2012, and from 5 to 20 February 2013, we, however, observed different depletion events. While atmospheric Hg(0) concentrations dropped and remained low (0.39 ± 0.19 ng/m^3 from 19 January to 8 February 2012, 0.41 ± 0.21 ng/m^3 from 5 to 20 February 2013) for several weeks (see Figs. 3a, 11a, and 11e), O_3 showed no abnormal variability (see Figs. 11d and 11h). These depletion events occurred as air masses stagnated over the Antarctic plateau (see Figs. 10a and 10b) according to our FLEXPART simulations. This stagnation of air masses is confirmed in 2013 (see Figs. 11f and 11g) by a decrease of

Atmos. Chem. Phys. Discuss., doi:10.5194/acp-2016-144, 2016
Manuscript under review for journal Atmos. Chem. Phys.
Published: 18 February 2016

temperature at 10 m a.g.l (from -29 ± 3 °C in January to -43 ± 4 °C during the Hg(0) depletion event) and a low integrated water vapor (0.40 ± 0.13 kg/m^2 during the Hg(0) depletion event vs. 0.77 ± 0.20 kg/m^2 in January). In both 2012 and 2013, depletions of Hg(0) ended when air masses started moving out of the plateau (see Figs. 10c and 10d).

While previous studies attributed high Hg(II) concentrations in the Antarctic summer to subsiding upper tropospheric air (Holmes et al., 2006; Brooks et al., 2008), potential emission sensitivities suggest that these depletions of Hg(0) were unlikely concomitant with upper troposphere/lower stratosphere intrusions (see Figs. 10a and 10b, PES at 4-10 km). This is also confirmed by stable O_3 mixing ratios. High altitude vertical profiles of Hg(0) should be carried out to rule out this hypothesis of subsiding upper tropospheric air. We suggest that these Hg(0) depletion events observed at Concordia Station result from processes occurring within the shallow boundary layer. Since O_3 was not depleted during these events, Hg(0) depletion cannot be accounted for by bromine oxidation alone. FLEXPART simulations along with integrated water vapor and temperature measurements indicate that these Hg(0) depletion events occurred as air masses stagnated over the Antarctic plateau. As highlighted in section 3.2, the oxidative capacity is high in summer on the plateau (Davis et al., 2001; Grannas et al., 2007; Eisele et al., 2008; Kukui et al., 2014). This air mass stagnation might favor an accumulation of oxidants within the shallow boundary layer (< 300 m in average), leading to an oxidation of Hg(0) stronger than usual.

3.6 Decreasing trend in winter

While stable concentrations were expected in winter given the absence of photochemistry, our observations reveal a 20 to 30% decrease of atmospheric Hg(0) concentrations from May to mid-August (see Fig. 3a). Conversely, Hg(0) concentrations remained stable at Troll and Neumayer from late fall through winter (Ebinghaus et al., 2002; Pfaffhuber et al., 2012). This decreasing trend observed in winter might be due to several mechanisms, including gas-phase oxidation and heterogeneous reactions.

3.6.1 Hypothesis on a gas-phase reaction

Several studies suggested the involvement of nitrate radicals in the night-time oxidation of Hg(0) (Mao and Talbot, 2012; Peleg et al., 2015). However, as previously mentioned, Dibble et al. (2012) indicated that NO_3 bound Hg(0) too weakly to initiate its oxidation in the gas phase. Another potential oxidant is O_3, with this reactant reaching a maximum in the winter

Atmos. Chem. Phys. Discuss., doi:10.5194/acp-2016-144, 2016
Manuscript under review for journal Atmos. Chem. Phys.
Published: 18 February 2016

(Legrand et al., 2009). However, according to some theoretical studies (e.g., Hynes et al., 2009), reaction (R1) is unlikely to proceed as a homogeneous reaction. Several experimental studies confirmed the major product of reaction (R1) to be solid mercuric oxide, HgO (s) and not HgO (g) (e.g., Pal and Ariya, 2004; Ariya et al., 2009), suggesting that pure gas phase oxidation of elemental mercury by O_3 may not occur in the atmosphere. However, Calvert and Lindberg (2005) proposed an alternative mechanism that would make this reaction potentially viable in the atmosphere (Subir et al., 2011). The reaction may start with the formation of a metastable HgO_3 (g) molecule which then decomposes to OHgOO (g) and thereafter transforms to HgO (s) and O_2 (g).

$$Hg(0)\ (g) + O_3\ (g)\ \rightarrow HgO\ (g) + O_2\ (g) \quad \text{(R1)}$$

3.6.2 Influence of heterogeneous surfaces

As suggested by Subir et al. (2011), the influence of heterogeneous surfaces of water droplets, snow, ice and aerosols should be taken into account when attempting to describe mercury chemistry in the atmosphere. O'Concubhair et al. (2012) showed that freezing an acidic solution containing nitrite or hydrogen peroxide can oxidize dissolved gaseous mercury in the dark. Nitrous acid and hydrogen peroxide are present on the Antarctic plateau (Huey et al., 2004; Hutterli et al., 2004). As suggested by Dommergue et al. (2012), similar processes could occur in the snow or on surface hoar at Concordia Station in winter. In 2013, the height of measurement had a significant influence on the decline over time of Hg(0) concentrations (ANCOVA test, p value < 2.10^{-16}), with a steeper decrease at 25 cm than at 1070 cm. This result suggests that snowpack may act as a sink for mercury, enhancing the deposition rate due to heterogeneous reactions, through absorption of oxidation products, and/or physical sorption/condensation of Hg(0) on surface snow.

In spite of the observed decreasing trend of Hg(0) concentrations in ambient air, total mercury concentrations in surface snow samples did not significantly increase over time in winter (see Fig. 4). Using a snow density of 300 kg/m^3 a loss of 0.30 ng/m^3 over a period of three months in a mixing layer of 50 m high would lead to a 5.0 ng/L increase in the first cm of the snowpack. Given the variability of chemical species deposition onto the snow surface, and the occurrence of either fresh snowfall or blowing snow, this 5.0 ng/L increase over a period of three months could not be detected in our weekly surface snow samples.

Despite the overall decreasing trend in winter, Hg(0) concentration exhibited abrupt increases when moist and warm air masses from lower latitudes occasionally reached Concordia

Station. This is, for example, evidenced on 13 June 2012 by an increase of 0.25 ng/m^3 of the Hg(0) concentration, an increase of temperature at 10 m a.g.l. from -63 to -26 °C, and a high integrated water vapor column (see Fig. 12).

3.7 Implications at a continental scale

Depletion events of atmospheric Hg(0) that have been observed in the Artic and at various coastal Antarctic stations have been associated with O_3 depletions, where Hg(0) and O_3 concentrations are positively correlated (Simpson et al., 2007). Increases in both Hg(II) and Hg(p) have been reported in conjunction with decreases of Hg(0) (Lu et al., 2001; Lindberg et al., 2002; Aspmo et al., 2005). Conversely, low Hg(0) concentrations that were not correlated or anti-correlated with O_3 were observed at Neumayer and Troll (Temme et al., 2003; Pfaffhuber et al., 2012), while elevated Hg(II) concentrations (up to 0.33 ng/m^3) were recorded at Terra Nova Bay in the absence of Hg(0)/O_3 depletion (Sprovieri et al., 2002). The continuous oxidation of Hg(0) in summer (see section 3.2) and multi-day Hg(0) depletion events observed at Concordia Station in January/February (see section 3.5) are expected to result in the build-up of an inland atmospheric reservoir enriched in Hg(II) and depleted in Hg(0) in the summer. Due to strong katabatic winds flowing out from the Antarctic Plateau – generated by the negative buoyant force that develops in the stable cooled layer along the ice sheet slopes (Gallée and Pettré, 1998) –, a fraction of this inland atmospheric reservoir can be transported toward the coastal margin. The influence of the flows from the Antarctic plateau on coastal locations varies depending on the location. As demonstrated by Parish and Bromwich (1987) and Parish and Bromwich (2007), the volume of air moving off inland Antarctica toward the coastal margin displays significant spatial variability due to the topographic slope and orientation of the underlying ice sheets. Northward transport of air from the plateau is enhanced in a few locations called confluence zones – e.g., the broad region upslope from the Ross Ice Shelf at 175°E and the area near Adélie Land at 142°E (Parish and Bromwich, 1987, 2007) – but can be sporadically observed elsewhere explaining observations at Neumayer, Troll, or Terra Nova Bay (Temme et al., 2003; Sprovieri et al., 2002; Pfaffhuber et al., 2012). Monitoring atmospheric mercury at a coastal station situated close to a confluence zone could provide new insights regarding the extent of the transport of reactive air masses from the Antarctic plateau. This topic will be addressed in a companion papier (Angot et al., this issue). The Antarctic continent shelters unconventional atmospheric pathways of mercury reactivity both in winter and in summer. Its role should be taken into account in the modeling of the global geochemical cycle of mercury.

4 Conclusion

Mean summertime atmospheric Hg(0) concentration was ~ 25% lower compared to values recorded at other Antarctic stations at the same period of the year, suggesting a continuous oxidation of atmospheric Hg(0) within the shallow boundary layer as a result of the high oxidative capacity of the Antarctic plateau atmosphere at this period of the year. This hypothesis is further supported by high total mercury concentrations in surface snow samples measured at the station (up to 74 ng/L). Our results confirm short-term observations by Brooks et al. (2008) and Dommergue et al. (2012) of chemical exchange at the air/snow interface. During the sunlit period, Hg(0) concentration peaked in the upper layers of the snowpack. Summertime Hg(0) concentration in ambient air exhibited a pronounced diurnal cycle likely due to large emissions from the snowpack as a response to daytime heating. Our observations also reveal a decrease of atmospheric mercury concentrations in winter (24-h darkness) likely due to a gas-phase oxidation and/or heterogeneous reactions. Interestingly, this decreasing trend has never been observed elsewhere. Finally, we reveal the occurrence of multi-day to weeklong depletion events of Hg(0) in ambient air in summer, that are not associated with depletion of O_3, and likely result from a stagnation of air masses on the plateau triggering an accumulation of oxidants in the shallow boundary layer. This behaviour is radically different from what is usually observed in the Arctic where only mercury depletion events that were associated with O_3 depletion (and with a Hg(0)/O_3 correlation) have been highlighted so far. According to observations at coastal Antarctic stations, the reactivity observed at Concordia Station can be transported at a continental scale by strong katabatic winds. Our understanding of the atmospheric mercury chemistry on the Antarctic plateau is currently limited by the lack of continuous halogens measurements. Our findings point out new directions for future kinetic, observational, and modeling studies.

Acknowledgements

We thank A. Barbero and the rest of the overwintering crew: S. Aubin, C. Lenormant, and R. Jacob. We also gratefully acknowledge M. Barret for the development of a QA/QC software program, D. Liptzin for the calculation of the Obukhov length and friction velocity, M. Legrand for the 2012 ozone data, C. Genthon for the meteorological data, E. Vignon for helpful discussion, and B. Jourdain and X. Faïn for their help in the field. This work

contributed to the EU-FP7 project Global Mercury Observation System (GMOS – www.gmos.eu) and has been supported by a grant from Labex OSUG@2020 (Investissements d'avenir – ANR10 LABX56), and the Institut Universitaire de France. BQ and PR acknowledge ANR CLIMSLIP and HAMSTRAD Program 910, respectively. Logistical and financial support was provided by the French Polar Institute IPEV (Program 1028, GMOstral and Program 1011, SUNITEDC), and a grant from the U.S. National Science Foundation (NSF, PLR#1142145). Computing resources for FLEXPART simulations were provided by the IPSL CICLAD/CLIMSERV mesocenter. Meteorological data were obtained thanks to LEFE/IMAGO programs CLAPA and GABLS4, IPEV program CALVA/1013, and Observatoire des Sciences de l'Univers de Grenoble (GLACIOCLIM observatory).

Atmos. Chem. Phys. Discuss., doi:10.5194/acp-2016-144, 2016
Manuscript under review for journal Atmos. Chem. Phys.
Published: 18 February 2016

Atmospheric Chemistry and Physics Discussions

References

Anderson, P. S., and Neff, W. D.: Boundary layer physics over snow and ice, Atmospheric Chemistry and Physics, 8, 3563-3582, 2008.

Angot, H., Barret, M., Magand, O., Ramonet, M., and Dommergue, A.: A 2-year record of atmospheric mercury species at a background Southern Hemisphere station on Amsterdam Island, Atmospheric Chemistry and Physics 14, 11461-11473, 2014.

Angot, H., Dion, I., Vogel, N., Magand, O., Legrand, M., and Dommergue, A.: Atmospheric mercury record at Dumont d'Urville, East Antarctic coast: continental outflow and oceanic influences, Atmospheric Chemistry and Physics, this issue.

Argentini, S., Viola, A., Sempreviva, A. M., and Petenko, I.: Summer boundary-layer height at the plateau site of Dome C, Antarctica, Boundary-Layer Meteorology, 115, 409-422, 2005.

Argentini, S., Petenko, I., Viola, A., Mastrantonio, G., Pietroni, I., Casasanta, G., Aristidi, E., and Ghenton, C.: The surface layer observed by a high-resolution sodar at Dome C, Antarctica, Annals of geophysics, 56, doi:10.4401/ag-6347, 2013.

Ariya, P. A., Peterson, K., Snider, G., and Amyot, M.: Mercury chemical transformation in the gas, aqueous and heterogeneous phases: state-of-the-art science and uncertainties, in: Mercury fate and transport in the global atmosphere, edited by: Pirrone, N., and Mason, R. P., Springer, New York, 2009.

Aspmo, K., Gauchard, P.-A., Steffen, A., Temme, C., Berg, T., Bahlmann, E., Banic, C., Dommergue, A., Ebinghaus, R., Ferrari, C., Pirrone, N., Sprovieri, F., and Wibetoe, G.: Measurements of atmospheric mercury species during an international study of mercury depletion events at Ny-Ålesund, Svalbard, spring 2003. How reproductible are our present methods?, Atmospheric Environment, 39, 7607-7619, 2005.

Bloom, N. S., and Fitzgerald, W. F.: Determination of volatile mercury species at the picogram level by low temperature gas chromatography with cold-vapor atomic fluorescence detection, Analytica Chimica Acta, 208, 151-161, 1988.

Bocquet, F., Helmig, D., and Oltmans, S. J.: Ozone in interstitial air of the mid-latituden seasonal snowpack at Niwot Ridge, Colorado, Arctic, Antarctic, and Alpine Research, 39, 375-387, 2007.

Brooks, S., Saiz-Lopez, A., Skov, H., Lindberg, S. E., Plane, J. M. C., and Goodsite, M. E.: The mass balance of mercury in the springtime arctic environment, Geophysical research letters, doi: 10.1029/2005GL025525, 2006.

Brooks, S. B., Arimoto, R., Lindberg, S. E., and Southworth, G.: Antarctic polar plateau snow surface conversion of deposited oxidized mercury to gaseous elemental mercury with fractional long-term burial, Atmospheric Environment, 42, 2877-2884, 2008.

Calvert, J. G., and Lindberg, S. E.: Mechanisms of mercury removal by O_3 and OH in the atmosphere, Atmospheric Environment, 39, 3355-3367, 2005.

Cohen, L., Helmig, D., Neff, W. D., Grachev, A. A., and Fairall, C. W.: Boundary-layer dynamics and its influence on atmospheric chemistry at Summit, Greenland, Atmospheric Environment, 5044-5060, 2007.

D'Amore, F., Bencardino, M., Cinnirella, S., Sprovieri, F., and Pirrone, N.: Data quality through a web-based QA/QC system: implementation for atmospheric mercury data from the Global Mercury Observation System, Environmental Science: Processes & Impacts, 17, 1482-1491, 2015.

Davis, D., Nowak, J. B., Chen, G., Buhr, M., Arimoto, R., Hogan, A., Eisele, F., Mauldin, L., Tanner, D., Shetter, R., Lefer, B., and McMurry, P.: Unexpected high levels of NO observed at South Pole, Geophysical research letters, 28, 3625-3628, 2001.

Dibble, T. S., Zelie, M. J., and Mao, H.: Thermodynamics of reactions of ClHg and BrHg radicals with atmospherically abundant free radicals, Atmospheric Chemistry and Physics, 12, 10271-10279, 2012.

Domine, F., Albert, M., Huthwelker, T., Jacobi, H.-W., Kokhanovsky, A. A., Lehning, M., Picard, G., and Simpson, W. R.: Snow physics as relevant to snow photochemistry, Atmospheric Chemistry and Physics, 8, 171-208, 2008.

Dommergue, A., Ferrari, C. P., Poissant, L., Gauchard, P.-A., and Boutron, C. F.: Diurnal cycles of gaseous mercury within the snowpack at Kuujjuarapik/Whapmagoostui, Québec, Canada, Environmental Science and Technology, 37, 3289-3297, 2003.

Dommergue, A., Sprovieri, F., Pirrone, N., Ebinghaus, R., Brooks, S., Courteaud, J., and Ferrari, C. P.: Overview of mercury measurements in the antarctic troposphere, Atmospheric Chemistry and Physics, 10, 3309-3319, 2010.

Dommergue, A., Barret, M., Courteaud, J., Cristofanelli, P., Ferrari, C. P., and Gallée, H.: Dynamic recycling of gaseous elemental mercury in the boundary layer of the antarctic plateau, Atmospheric Chemistry and Physics, 12, 11027-11036, 2012.

Douglas, T. A., Sturm, M., Simpson, W. R., Blum, J. D., Alvarez-Aviles, L., Keeler, G. J., Perovich, D. K., Biswas, A., and Johnson, K.: Influence of snow and ice crystal formation and accumulation on mercury deposition to the Arctic, Environmental Science and Technology, 42, 1542-1551, 2008.

Driscoll, C. T., Mason, R. P., Chan, H. M., Jacob, D. J., and Pirrone, N.: Mercury as a global pollutant: sources, pathways, and effects, Environmental Science and Technology, 47, 4967-4983, 2013.

Durnford, D., and Dastoor, A.: The behavior of mercury in the cryosphere: a review of what we know from observations, Journal of geophysical research, 116, doi:10.1029/2010JD014809, 2011.

Ebinghaus, R., Kock, H. H., Temme, C., Einax, J. W., Löwe, A. G., Richter, A., Burrows, J. P., and Schroeder, W. H.: Antarctic springtime depletion of atmospheric mercury, Environmental Science and Technology, 36, 1238-1244, 2002.

Eisele, F., Davis, D. D., Helmig, D., Oltmans, S. J., Neff, W., Huey, G., Tanner, D., Chen, G., Crawford, J. H., Arimoto, R., Buhr, M., Mauldin, L., Hutterli, M., Dibb, J., Blake, D., Brooks, S. B., Johnson, B., Roberts, J. M., Wang, Y., Tan, D., and Flocke, F.: Antarctic tropospheric chemistry (ANTCI) 2003 overview, Atmospheric Environment, 2008, 2749-2761, 2008.

Faïn, X., Grangeon, S., Bahlmann, E., Fritsche, J., Obrist, D., Dommergue, A., Ferrari, C., Cairns, W., Ebinghaus, R., Barbante, C., Cescon, P., and Boutron, C. F.: Diurnal production of gaseous mercury in the alpine snowpack before snowmelt, Journal of geophysical research, 112, doi:10.1029/2007JD008520, 2007.

Faïn, X., Ferrari, C., Dommergue, A., Albert, M., Battle, M., Arnaud, L., Barnola, J.-M., Cairns, W., Barbante, C., and Boutron, C. F.: Mercury in the snow and firn at Summit Station, Central Greenland, and implications for the study of past atmospheric mercury levels, Atmospheric Chemistry and Physics, 8, 3441-3457, 2008.

Ferrari, C. P., Dommergue, A., Boutron, C. F., Skov, H., Goodsite, M. E., and Jensen, B.: Nighttime production of elemental gaseous mercury in interstitial air of snow at Station Nord, Greenland, Atmospheric Environment, 38, 2727-2735, 2004.

Ferrari, C. P., Gauchard, P.-A., Aspmo, K., Dommergue, A., Magand, O., Bahlmann, E., Nagorski, S., Temme, C., Ebinghaus, R., Steffen, A., Banic, C., Berg, T., Planchon, F., Barbante, C., Cescon, P., and Boutron, C. F.: Snow-to-air exchanges of mercury in an arctic seasonal snowpack in Ny-Alesund, Svalbard, Atmospheric Environment, 39, 7633-7645, 2005.

Ferrari, C. P., Padova, C., Faïn, X., Gauchard, P.-A., Dommergue, A., Aspmo, K., Berg, T., Cairns, W., Barbante, C., Cescon, P., Kaleschke, L., Richter, A., Wittrock, F., and Boutron, C. F.: Atmospheric mercury depletion event study in Ny-Alesund (Svalbard) in spring 2005.

Deposition and transformation of Hg in surface snow during springtime, Science of the Total Environment, 397, 167-177, 2008.

Fitzgerald, W. F., and Gill, G. A.: Subnanogram determination of mercury by two-stage gold amalgamation and gas detection applied to atmospheric analysis, Analytical chemistry, 51, 1714-1720, 1979.

France, J. L., King, M. D., Frey, M. M., Erbland, J., Picard, G., Preunkert, S., MacArthur, A., and Savarino, J.: Snow optical properties at Dome C (Concordia), Antarctica; implications for snow emissions and snow chemistry of reactive nitrogen, Atmospheric Chemistry and Physics, 11, 9787-9801, 2011.

Frey, M. M., Brough, N., France, J. L., Anderson, P. S., Traulle, O., King, M. D., Jones, A. E., Wolff, E. W., and Savarino, J.: The diurnal variability of atmospheric nitrogen oxides (NO and NO2) above the Antarctic Plateau driven by atmospheric stability and snow emissions, Atmospheric Chemistry and Physics, 13, 3045-3062, 2013.

Frey, M. M., Roscoe, H. K., Kukui, A., Savarino, J., France, J. L., King, M. D., Legrand, M., and Preunkert, S.: Atmospheric nitrogen oxides (NO and NO_2) at Dome C, East Antarctica, during the OPALE campaign, Atmospheric Chemistry and Physics, 15, 7859-7875, 2015.

Gallée, H., and Pettré, P.: Dynamical constraints on katabatic wind cessation in Adélie Land, Antarctica, Journal of the atmospheric sciences, 55, 1755-1770, 1998.

Gallée, H., and Gorodetskaya, I. V.: Validation of a limited area model over Dome C, Antarctic Plateau, during winter, Climate Dynamics, 34, 61-72, 2010.

Gallée, H., Preunkert, S., Argentini, S., Frey, M. M., Genthon, C., Jourdain, B., Pietroni, I., Casasanta, G., Barral, H., Vignon, E., Amory, C., and Legrand, M.: Characterization of the boundary layer at Dome C (East Antarctica) during the OPALE summer campaign, Atmospheric Chemistry and Physics, 15, 6225-6236, 2015.

Genthon, C., Town, M. S., Six, D., Favier, V., Argentini, S., and Pellegrini, A.: Meteorological atmospheric boundary layer measurements and ECMWF analyses during summer at Dome C, Antarctica, Journal of geophysical research, 115, D05104, 2010.

Genthon, C., Six, D., Gallée, H., Grigioni, P., and Pellegrini, A.: Two years of atmospheric boundary layer observations on a 45-m tower at Dome C on the Antarctic plateau, Journal of geophysical research: atmospheres, 118, 3218-3232, 2013.

Goodsite, M. E., Plane, J. M. C., and Skov, H.: A theoretical study of the oxidation of Hg^0 to $HgBr_2$ in the troposphere, Environmental Science and Technology, 38, 1772-1776, 2004.

Grannas, A. M., Jones, A. E., Dibb, J., Ammann, M., Anastasio, C., Beine, H. J., Bergin, M., Bottenheim, J., Boxe, C. S., Carver, G., Chen, G., Crawford, J. H., Domine, F., Frey, M. M., Guzman, M. I., Heard, D. E., Helmig, D., Hoffmann, M. R., Honrath, R. E., Huey, L. G., Hutterli, M., Jacobi, H.-W., Klan, P., Lefer, B., McConnell, J. R., Plane, J. M. C., Sander, R., Savarino, J., Shepson, P. B., Simpson, W. R., Sodeau, J., Von Glasow, R., Weller, R., Wolff, E. W., and Zhu, T.: An overview of snow photochemistry: evidence, mechanisms and impacts, Atmospheric Chemistry and Physics, 7, 4329-4373, 2007.

Hedgecock, I. M., and Pirrone, N.: Chasing quicksilver: modeling the atmospheric lifetime of Hg(0) in the marine boundary layer at various latitudes, Environmental Science and Technology, 38, 69-76, 2004.

Hoegstroem, U.: Non-dimensional wind and temperature profiles in the atmosphere surface layer: a re-evaluation, Boundary-Layer Meteorology, 42, 55-78, 1988.

Holmes, C. D., Jacob, D. J., and Yang, X.: Global lifetime of elemental mercury against oxidation by atomic bromine in the free troposphere, Geophysical research letters, 33, 2006.

Huey, L. G., Tanner, D. J., Slusher, D. L., Dibb, J. E., Arimoto, R., Chen, G., Davis, D., Buhr, M. P., Nowak, J. B., Mauldin, L., Eisele, F. L., and Kosciuch, E.: CIMS measurements of

HNO_3 and SO_2 at the South Pole during ISCAT 2000, Atmospheric Environment, 38, 5411-5421, 2004.

Hutterli, M. A., McConnell, J. R., Chen, G., Bales, R. C., Davis, D. D., and Lenschow, D. H.: Formaldehyde and hydrogen peroxide in air, snow and intersitial air at South Pole, Atmospheric Environment, 38, 5439-5450, 2004.

Hynes, A. J., Donohoue, D. L., Goodsite, M. E., and Hedgecock, I. M.: Our current understanding of major chemical and physical processes affecting mercury dynamics in the atmosphere and at the air-water/terrestrial interfaces, in: Mercury fate and transport in the global atmosphere, edited by: Pirrone, N., and Mason, R. P., Springer, New York, 427-457, 2009.

Johnson, K. P., Blum, J. D., Keeler, G. J., and Douglas, T. A.: Investigation of the deposition and emission of mercury in arctic snow during an atmospheric mercury depletion event, Journal of geophysical research, 113, doi: 10.1029/2008JD009893, 2008.

Kerbrat, M., Legrand, M. P., S., Gallée, H., and Kleffmann, J.: Nitrous acid at Concordia (inland site) and Dumont d'Urville (coastal site), east antarctica, Journal of geophysical research, 117, doi:10.1029/2011JD017149, 2012.

King, J. C., and Anderson, P. S.: Heat and water vapor fluxes and scalar roughness lengths over an Antarctic ice shelf, Boundary-Layer Meteorology, 69, 101-121, 1994.

King, J. C., Argentini, S. A., and Anderson, P. S.: Contrasts between the summertime surface energy balance and boundary layer structure at Dome C and Halley stations, Antarctica, Journal of geophysical research, 111, doi:10.1029/2005JD006130, 2006.

King, M. D., and Simpson, W. R.: Extinction of UV radiation in Arctic snow at Alert, Canada (82°N), Journal of geophysical research 106, 12499-12507, 2001.

Kukui, A., Legrand, M., Preunkert, S., Frey, M. M., Loisil, R., Gil Roca, J., Jourdain, B., King, M. D., France, J. L., and Ancellet, G.: Measurements of OH and RO_2 radicals at Dome C, East Antarctica, Atmospheric Chemistry and Physics, 14, 12373-12392, 2014.

Lalonde, J. D., Amyot, M., Doyon, M.-R., and Auclair, J.-C.: Photo-induced Hg(II) reduction in snow from the remote and temperate experimental lakes area (Ontario, Canada), Journal of geophysical research, 108, doi:10.1029/2001JD001534, 2003.

Legrand, M., Preunkert, S., Jourdain, B., Gallée, H., Goutail, F., Weller, R., and Savarino, J.: Year-round record of surface ozone at coastal (Dumont d'Urville) and inland (Concordia) sites in east antarctica, Journal of geophysical research, 114, doi:10.1029/2008JD011667, 2009.

Legrand, M. P., S., Savarino, J., Frey, M. M., Kukui, A., Helmig, D., Jourdain, B., Jones, A., Weller, R., Brough, N., and Gallée, H.: Inter-annual variability of surface ozone at coastal (Dumont d'Urville, 2004-2014) and inland (Concordia, 2007-2014) sites in East Antarctica, Submitted to ACP.

Lin, C.-J., and Pehkonen, S. O.: The chemistry of atmospheric mercury: a review, Atmospheric Environment, 33, 2067-2079, 1999.

Lin, C.-J., Pan, L., Streets, D. G., Shetty, S. K., Jang, C., Feng, X., Chu, H.-W., and Ho, T. C.: Estimating mercury emission outflow from East Asia using CMAQ-Hg, Atmospheric Chemistry and Physics, 10, 1856-1864, 2010.

Lindberg, S. E., Brooks, S., Lin, C.-J., Scott, K. J., Landis, M. S., Stevens, R. K., Goodsite, M. E., and Richter, A.: Dynamic oxidation of gaseous mercury in the arctic troposphere at polar sunrise, Environmental Science and Technology, 36, 1245-1256, 2002.

Lu, J. Y., Schroeder, W. H., Barrie, L. A., Steffen, A., Welch, H. E., Martin, K., Lockhart, L., Hunt, R. V., Boila, G., and Richter, A.: Magnification of atmospheric mercury deposition to polar regions in springtime: the link to tropospheric ozone depletion chemistry, Geophysical research letters, 28, 3219-3222, 2001.

Mao, H., and Talbot, R.: Speciated mercury at marine, coastal, and inland sites in New England - Part 1: Temporal variability, Atmospheric Chemistry and Physics, 12, 5099-5112, 2012.

Mason, R. P., Choi, A. L., Fitzgerald, W. F., Hammerschmidt, C. R., Lamborg, C. H., Soerensen, A. L., and Sunderland, E. M.: Mercury biogeochemical cycling in the ocean and policy implications, Environmental Research, 119, 101-117, 2012.

Munthe, J., Sprovieri, F., Horvat, M., and Ebinghaus, R.: SOPs and QA/QC protocols regarding measurements of TGM, GEM, RGM, TPM and mercury in precipitation in cooperation with WP3, WP4 and WP5. GMOS deliverable 6.1, CNR-IIA, IVL. http://www.gmos.eu, last access: 3 March 2014, 2011.

Neff, W., Helmig, D., Grachev, A. A., and Davis, D.: A study of boundary layer behavior associated with high NO concentrations at the South Pole using a minisodar, tethered balloon, and sonic anemometer, Atmospheric Environment, 42, 2762-2779, 2008.

O'Concubhair, R., O'Sullivan, D. A., and Sodeau, J. R.: Dark oxidation of dissolved gaseous mercury in polar ice mimics, Environmental Science and Technology, 46, 2012.

Pal, B., and Ariya, P. A.: Studies of ozone initiated reactions of gaseous mercury: kinetics, product studies, and atmospheric implications, Physical Chemistry Chemical Physics, 6, 572-579, 2004.

Parish, T. R., and Bromwich, D. H.: The surface windfield over the Antarctic ice sheets, Nature, 328, 51-54, 1987.

Parish, T. R., and Bromwich, D. H.: Reexamination of the near-surface airflow over the Antarctic continent and implications on atmospheric circulations at high southern latitudes, Monthly Weather Review, 135, 1961-1973, 2007.

Peleg, M., Tas, E., Obrist, D., Matveev, V., Moore, C., Gabay, M., and Luria, M.: Observational evidence for involvement of nitrate radicals in nighttime oxidation of mercury, Environmental Science and Technology, 49, 14008-14018, 2015.

Perovich, D. K.: Light reflection and transmission by a temperate snow cover, Journal of glaciology, 53, 201-210, 2007.

Pfaffhuber, K. A., Berg, T., Hirdman, D., and Stohl, A.: Atmospheric mercury observations from Antarctica: seasonal variation and source and sink region calculations, Atmospheric Chemistry and Physics, 12, 3241-3251, 2012.

Pietroni, I., Argentini, S., Petenko, I., and Sozzi, R.: Measurements and parametrizations of the atmospheric boundary-layer height at Dome C, Antarctica, Boundary-Layer Meteorology, 143, 189-206, 2012.

Ricaud, P., Grigioni, P., Zbinden, R., Attié, J.-L., Genoni, L., Galeandro, A., Moggio, L., Montaguti, S., Petenko, I., and Legovini, P.: Review of tropospheric temperature, absolute humidity and integrated water vapor from the HAMSTRAD radiometer installed at Dome C, Antarctica, 2009-14, Antarctic Science, 27, 598-616, 2015.

Schroeder, W. H., Anlauf, K. G., Barrie, L. A., Lu, J. Y., Steffen, A., Schneeberger, D. R., and Berg, T.: Arctic spingtime depletion of mercury, Nature, 394, 331-332, 1998.

Seok, B., Helmig, D., Williams, M. W., Liptzin, D., and Chowanski, K. H., J.: An automated system for continuous measurements of trace gas fluxes through snow: an evaluation of the gas diffusion method at a subalpine forest site, Niwot Ridge, Colorado, Biogeochemistry, 95, 95-113, 2009.

Simpson, W. R., Von Glasow, R., Riedel, K., Anderson, P. S., Ariya, P. A., Bottenheim, J., Burrows, J. P., Carpenter, L. J., Friess, U., Goodsite, M. E., Heard, D. E., Hutterli, M., Jacobi, H.-W., Kaleschke, L., Neff, W., Plane, J. M. C., Platt, U., Richter, A., Roscoe, H. K., Sander, R., Shepson, P. B., Sodeau, J., Steffen, A., Wagner, T., and Wolff, E. W.: Halogens and their

role in polar boundary-layer ozone depletion, Atmospheric Chemistry and Physics, 7, 4375-4418, 2007.

Slemr, F., Angot, H., Dommergue, A., Magand, O., Barret, M., Weigelt, A., Ebinghaus, R., Brunke, E.-G., Pfaffhuber, K. A., Edwards, G., Howard, D., Powell, J., Keywood, M., and Wang, F.: Comparison of mercury concentrations measured at several sites in the Southern Hemisphere, Atmospheric Chemistry and Physics, 15, 3125-3133, 2015.

Sprovieri, F., Pirrone, N., Hedgecock, I. M., Landis, M. S., and Stevens, R. K.: Intensive atmospheric mercury measurements at Terra Nova Bay in antarctica during November and December 2000, Journal of geophysical research, 107, 4722, 2002.

Steffen, A., Schroeder, W., Bottenheim, J., Narayan, J., and Fuentes, J. D.: Atmospheric mercury concentrations: measurements and profiles near snow and ice surfaces in the Canadian Arctic during Alert 2000, Atmospheric Environment, 36, 2653-2661, 2002.

Steffen, A., Douglas, T., Amyot, M., Ariya, P. A., Aspmo, K., Berg, T., Bottenheim, J., Brooks, S., Cobbett, F., Dastoor, A., Dommergue, A., Ebinghaus, R., Ferrari, C., Gardfeldt, K., Goodsite, M. E., Lean, D., Poulain, A. J., Scherz, C., Skov, H., Sommar, J., and Temme, C.: A synthesis of atmospheric mercury depletion event chemistry in the atmosphere and snow, Atmospheric Chemistry and Physics, 8, 1445-1482, 2008.

Steffen, A., Scherz, T., Oslon, M., Gay, D. A., and Blanchard, P.: A comparison of data quality control protocols for atmospheric mercury speciation measurements, Journal of Environmental Monitoring, 14, 752-765, doi: 10.1039/c2em10735j, 2012.

Stohl, A., Hittenberger, M., and Wotawa, G.: Validation of the Lagrangian particle dispersion model FLEXPART against large scale tracer experiments, Atmospheric Environment, 32, 4245-4264, 1998.

Stohl, A., and Thomson, D. J.: A density correction for Lagrangian particle dispersion models, Boundary-Layer Meteorology, 90, 155-167, 1999.

Stohl, A., Forster, C., Frank, A., Seibert, P., and Wotawa, G.: Technical note: the Lagrangian particle dispersion model FLEXPART version 6.2, Atmospheric Chemistry and Physics, 5, 2461-2474, 2005.

Subir, M., Ariya, P. A., and Dastoor, A.: A review of uncertainties in atmospheric modeling of mercury chemistry I. Uncertainties in existing kinetic parameters - fundamental limitations and the importance of heteregeneous chemistry, Atmospheric Environment, 45, 5664-5675, 2011.

Tekran: Tekran 2537 mercury monitor detection limit. Summary of known estimates, Tekran Instruments Corp., Toronto, ON, Canada., 2011.

Temme, C., Einax, J. W., Ebinghaus, R., and Schroeder, W. H.: Measurements of atmospheric mercury species at a coastal site in the antarctic and over the atlantic ocean during polar summer, Environmental Science and Technology, 37, 22-31, 2003.

UNEP: Text of the Minamata Convention on Mercury for adoption by the Conference of Plenipotentiaries. unep.org. July 31, Available at: http://www.unep.org/hazardoussubstances/Portals/9/Mercury/Documents/dipcon/CONF_3_Minamata%20Convention%20on%20Mercury_final%2026%2008_e.pdf, last access: 28 February 2014, 2013.

Wang, F., Saiz-Lopez, A., Mahajan, A. S., Gomez Martin, J. C., Armstrong, D., Lemes, M., Hay, T., and Prados-Roman, C.: Enhanced production of oxidised mercury over the tropical pacific ocean: a key missing oxidation pathway, Atmospheric Chemistry and Physics, 14, 1323-1335, 2014.

Weiss-Penzias, P., Jaffe, D. A., Swartzendruber, P., Hafner, W., Chand, D., and Prestbo, E.: Quantifying Asian and biomass burning sources of mercury using the Hg/CO ratio in pollution plumes observed at the Mount Bachelor observatory, Atmospheric Environment, 41, 4366-4379, 2007.

Atmos. Chem. Phys. Discuss., doi:10.5194/acp-2016-144, 2016
Manuscript under review for journal Atmos. Chem. Phys.
Published: 18 February 2016

Xiao, W., Liu, S., Li, H., Xiao, Q., Wang, W., Hu, Z., Hu, C., Gao, Y., Shen, J., Zhao, X., Zhang, M., and Lee, X.: A flux-gradient system for simultaneous measurement of the CH_4, CO_2, and H_2O fluxes at a lake-air interface, Environmental Science and Technology, 48, 14490-14498, 2014.

Atmos. Chem. Phys. Discuss., doi:10.5194/acp-2016-144, 2016
Manuscript under review for journal Atmos. Chem. Phys.
Published: 18 February 2016

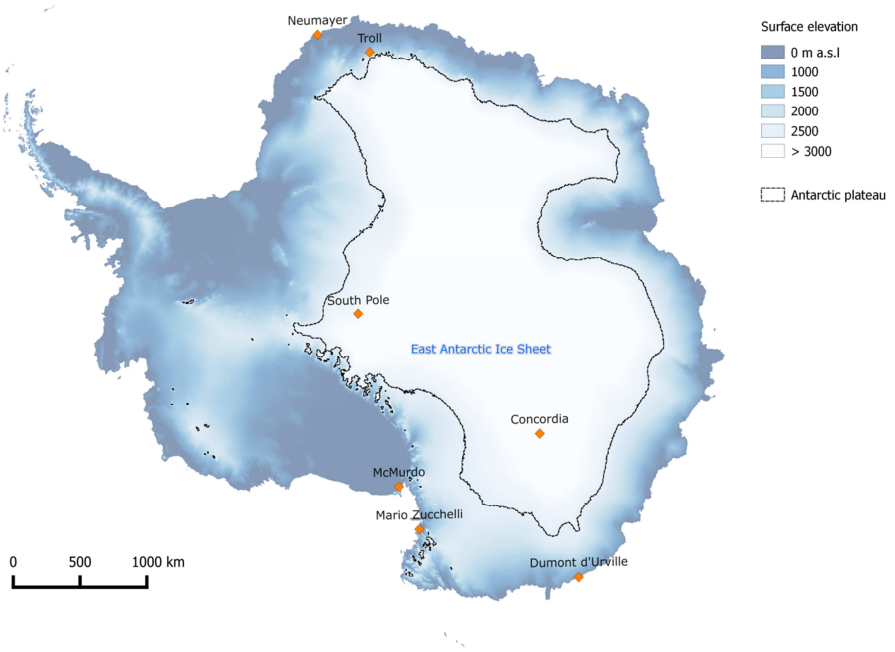

Figure 1: Map of Antarctica showing surface elevation (meters above sea level, m a.s.l) and the position of stations where atmospheric mercury measurements have been performed with modern on-line instruments. The black line shows the periphery of the high altitude plateau (> 2500 m a.s.l).

Atmos. Chem. Phys. Discuss., doi:10.5194/acp-2016-144, 2016
Manuscript under review for journal Atmos. Chem. Phys.
Published: 18 February 2016

a)

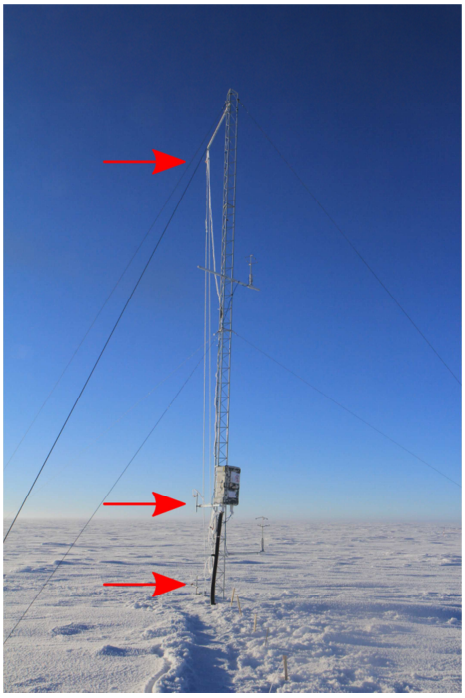

b)

Figure 2: Photographs showing **a)** the meteorological tower with the three gas inlets (red arrows) at 1070 cm, 210 cm and 25 cm above the snow surface (photo credit: B. Jourdain), and **b)** one of the snow towers with the two sampling inlets above the snowpack at 50 and 10 cm (photo credit: D. Helmig) .

Atmos. Chem. Phys. Discuss., doi:10.5194/acp-2016-144, 2016
Manuscript under review for journal Atmos. Chem. Phys.
Published: 18 February 2016

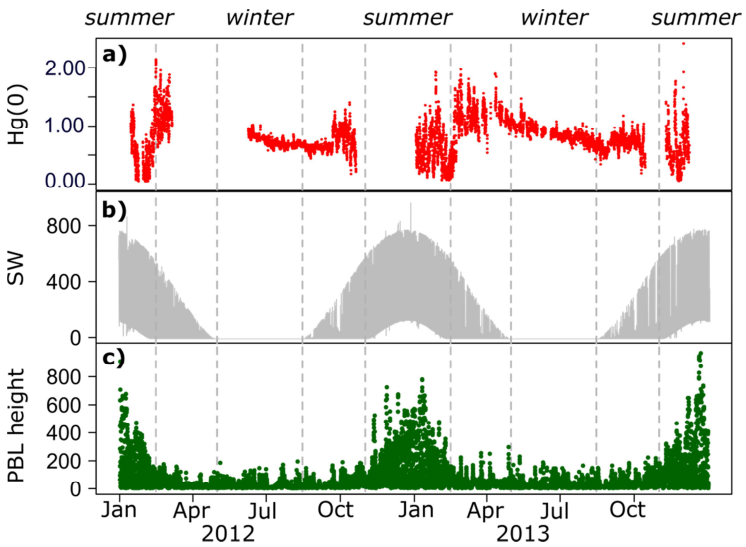

Figure 3: Annual variation in 2012 and 2013 of **a)** hourly-averaged Hg(0) concentrations (in ng/m^3) at 500 cm and 25 cm above the snow surface in 2012 and 2013, respectively, **b)** downwelling shortwave (SW) radiation (in W/m^2), and **c)** planetary boundary layer (PBL) height (in m). The vertical dashed lines represent seasonal boundaries.

Atmos. Chem. Phys. Discuss., doi:10.5194/acp-2016-144, 2016
Manuscript under review for journal Atmos. Chem. Phys.
Published: 18 February 2016

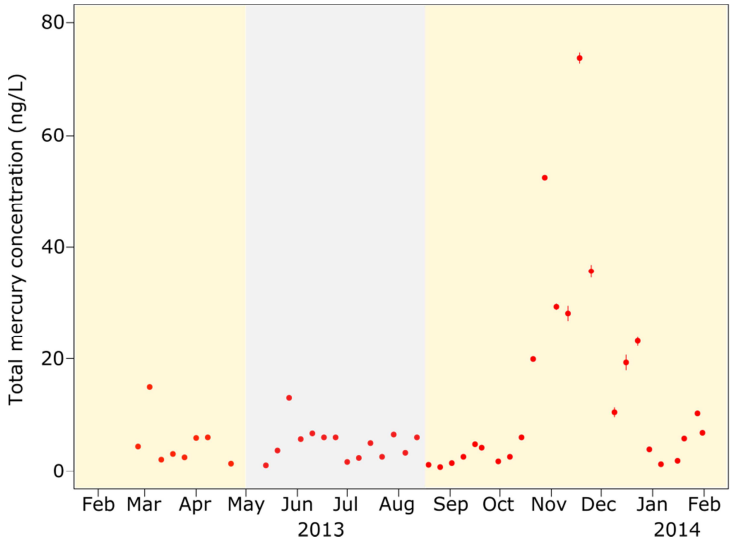

Figure 4: Total mercury concentration (ng/L), along with standard errors, in surface snow samples collected weekly at Concordia Station from February 2013 to January 2014. Dark period (winter) highlighted in grey, sunlit period highlighted in yellow. Total mercury concentrations were elevated (up to 74 ng/L) in November-December 2013 (summer).

Atmos. Chem. Phys. Discuss., doi:10.5194/acp-2016-144, 2016
Manuscript under review for journal Atmos. Chem. Phys.
Published: 18 February 2016

Atmospheric Chemistry and Physics Discussions
Open Access
EGU

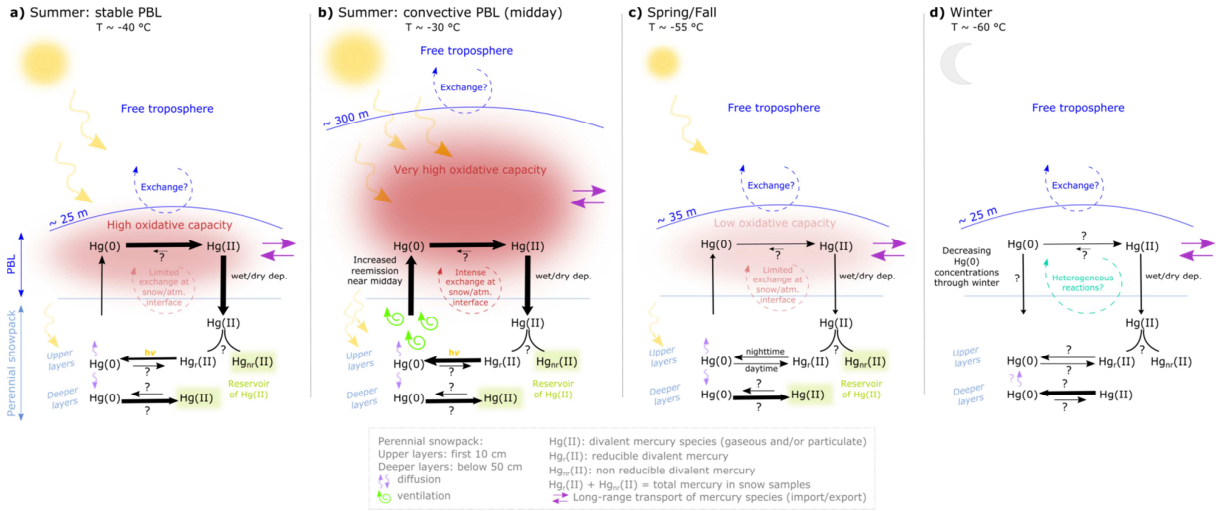

Figure 5: Schematic diagram illustrating the processes that govern the Hg(0) budget at Concordia Station **a)** in summer under stable Planetary Boundary Layer (PBL) conditions, **b)** in summer under convective PBL conditions, **c)** in spring/fall, and **d)** in winter. In summer, Hg(0) is continuously oxidized due to the high oxidative capacity of the boundary layer and a large amount of divalent mercury species deposit onto the snowpack. A fraction of deposited mercury can be reduced (the reducible pool, Hg$_r$(II)) in the upper layers of the snowpack and subsequently reemitted to the atmosphere as Hg(0). Hg(0) emission from the snowpack maximizes near midday likely due to increased ventilation as a response to daytime heating. Oxidation of Hg(0) dominates in the deeper layers of the snowpack leading to the formation of a Hg(II) reservoir. In spring/fall, the balance of reduction and oxidation processes within the upper layers of the snowpack differs from summertime: oxidation dominates during the day, reduction at night. In winter, Hg(0) is produced in the deeper layers of the snowpack likely as a result of the reduction of Hg(II) species accumulated during the sunlit period. Ambient Hg(0) concentrations exhibit a 20 to 30% decrease through winter.

Atmos. Chem. Phys. Discuss., doi:10.5194/acp-2016-144, 2016
Manuscript under review for journal Atmos. Chem. Phys.
Published: 18 February 2016

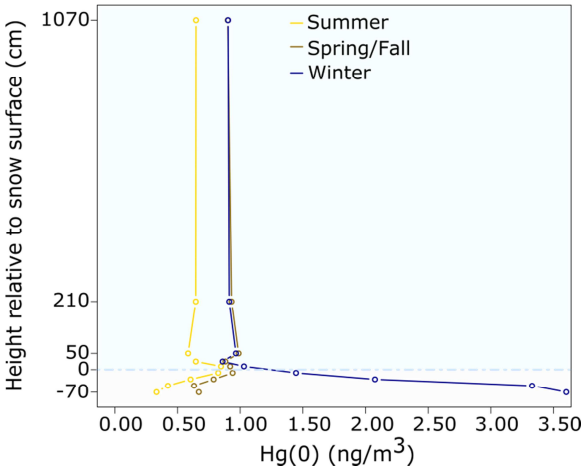

Figure 6: Mean Hg(0) concentration (ng/m^3) measured at various heights above and below the snow surface (cm) at Concordia Station in summer (yellow), spring/fall (brown), and winter (dark blue) The horizontal light blue dashed line represents the snow surface.

Atmos. Chem. Phys. Discuss., doi:10.5194/acp-2016-144, 2016
Manuscript under review for journal Atmos. Chem. Phys.
Published: 18 February 2016

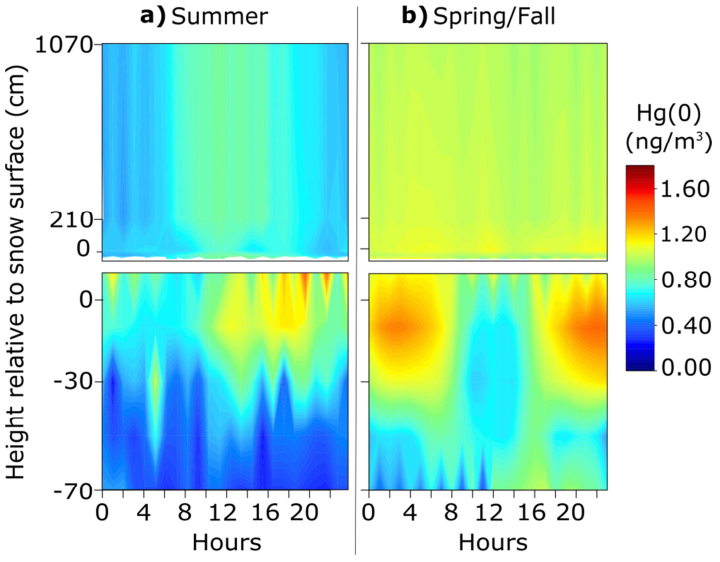

Figure 7: Hourly (local time) mean atmospheric and interstitial air Hg(0) concentrations in **a)** summer, and **b)** spring/fall. The vertical axis is the height of measurement relative to the snow surface (in cm). Color contours show Hg(0) concentrations (in ng/m^3).

Atmos. Chem. Phys. Discuss., doi:10.5194/acp-2016-144, 2016
Manuscript under review for journal Atmos. Chem. Phys.
Published: 18 February 2016

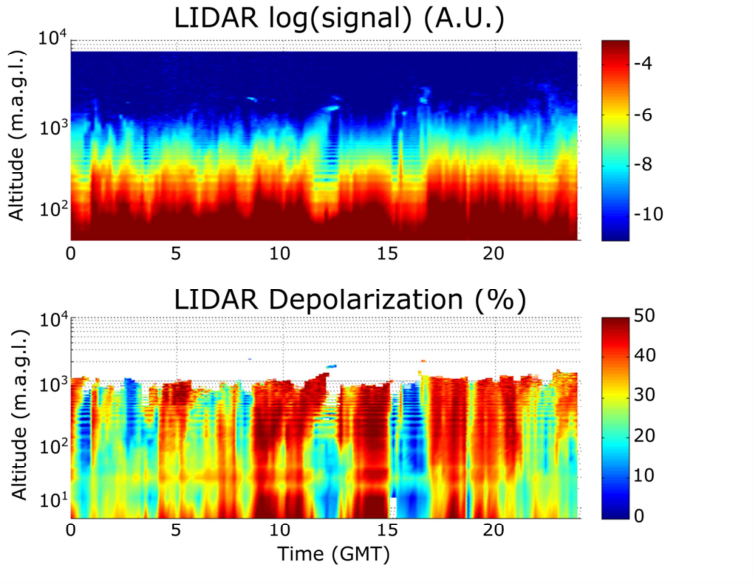

Figure 8: Lidar backscatter (upper panel) and depolarization ratio (lower panel) measured at Concordia Station on 24 February 2013. Ice precipitation was observed in the first 1000 m of the atmosphere, with only two small liquid-water clouds around 8 and 12 UTC.

Atmos. Chem. Phys. Discuss., doi:10.5194/acp-2016-144, 2016
Manuscript under review for journal Atmos. Chem. Phys.
Published: 18 February 2016

Atmospheric Chemistry and Physics Discussions
Open Access

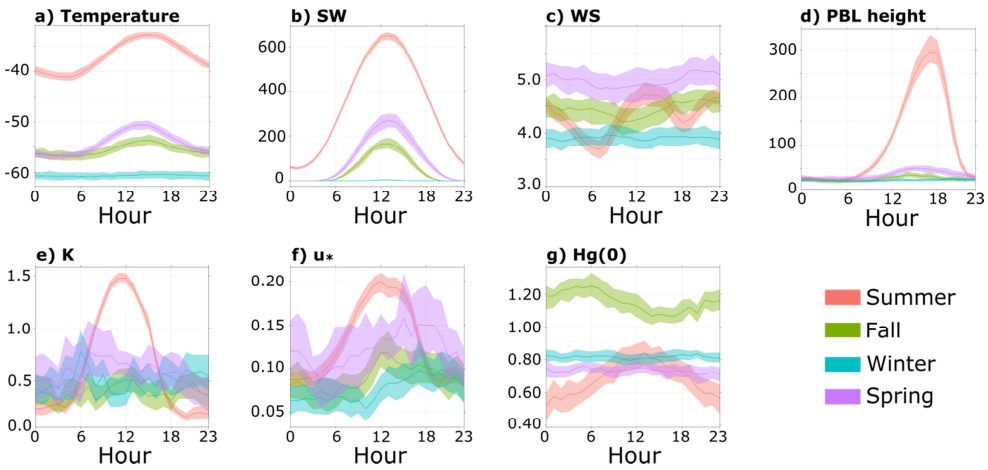

Figure 9: Hourly (local time) mean variation, along with the 95% confidence interval for the mean, of: **a)** temperature (in °C) at 3 m above the snow surface, **b)** downwelling shortwave (SW) radiation (in W/m^2) according to the MAR model simulations, **c)** wind speed at 3 m above the snow surface (in m/s), **d)** planetary boundary layer (PBL) height (in m) according to the MAR model simulations, **e)** Eddy diffusivity (K, in m^2/s), **f)** friction velocity (u_*, in m/s), and **g)** Hg(0) concentration (in ng/m^3), in summer (red), fall (green), winter (blue), and spring (purple).

Atmos. Chem. Phys. Discuss., doi:10.5194/acp-2016-144, 2016
Manuscript under review for journal Atmos. Chem. Phys.
Published: 18 February 2016

Atmospheric Chemistry and Physics
Discussions

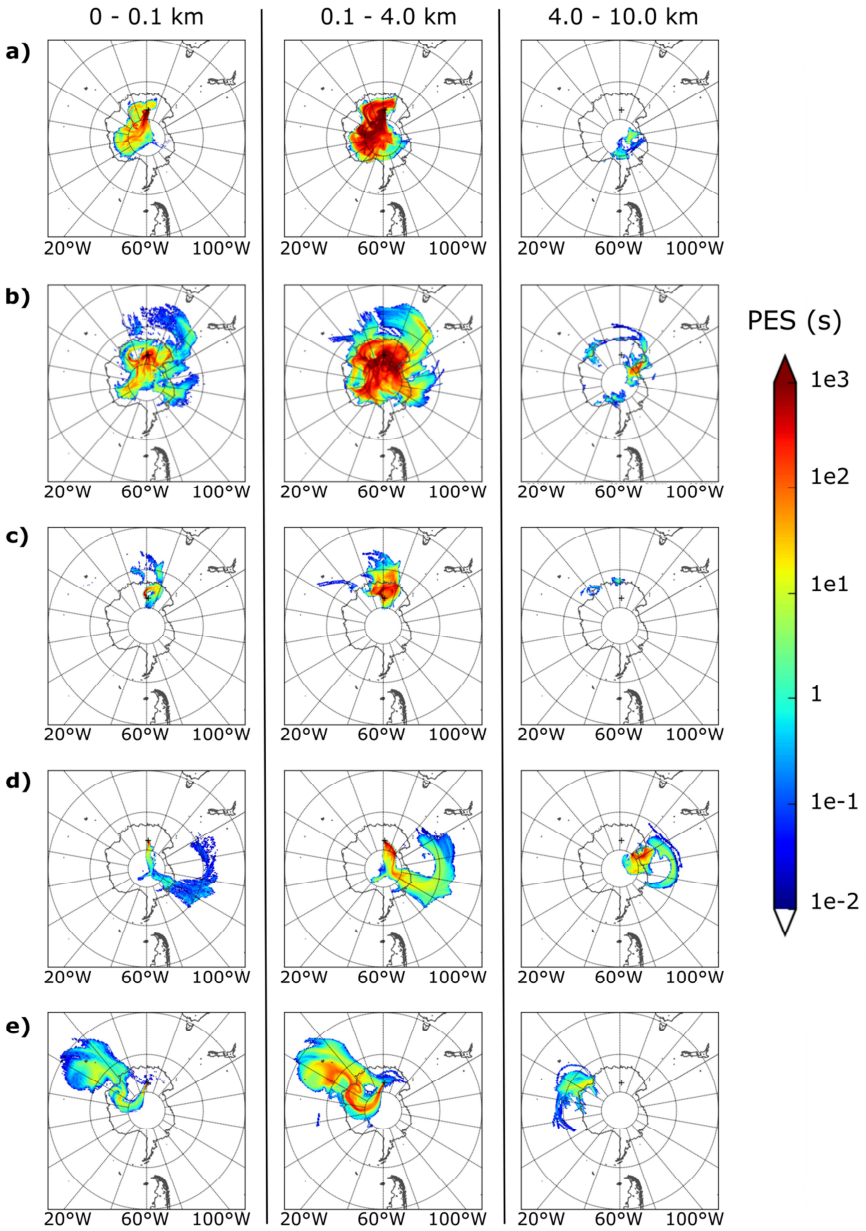

Figure 10: Back trajectories for the 3 layers of altitude colored according to the potential emission sensitivity (PES, in seconds) **a)** from 19 January to 8 February 2012, **b)** from 5 to 20 February 2013, **c)** on 10 February 2012, **d)** on 22 February 2013, and **e)** on 11 September 2013. Note that PES in a particular grid cell is proportional to the particle residence time in that cell.

Atmos. Chem. Phys. Discuss., doi:10.5194/acp-2016-144, 2016
Manuscript under review for journal Atmos. Chem. Phys.
Published: 18 February 2016

Atmospheric Chemistry and Physics
Discussions

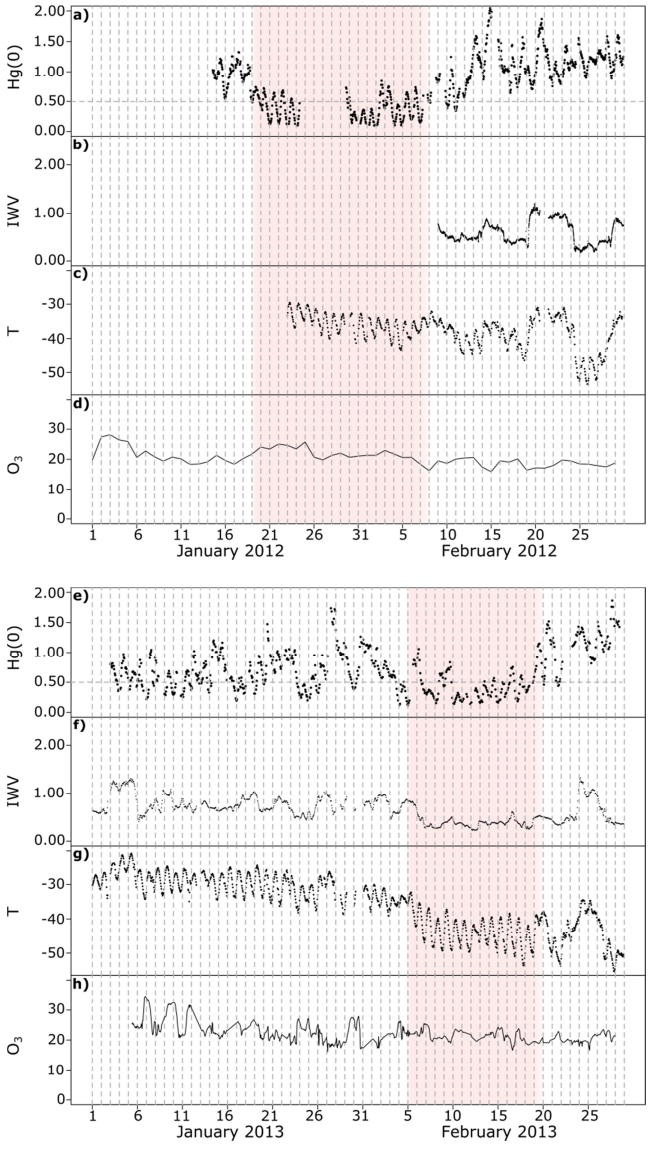

Figure 11: Top: January and February 2012 cycle of: **a)** hourly-averaged Hg(0) concentrations (in ng/m^3), **b)** Integrated Water Vapor (IWV, kg/m^2), **c)** Temperature (in °C) at 10 m above ground level, and **d)** ozone (O_3, daily mean) mixing ratios (ppbv). Hg(0) was low from 19 January to 8 February (period highlighted in red) while O_3 showed no abnormal variability. Bottom: January and February 2013 cycle of: **e)** hourly-averaged Hg(0) concentrations (in ng/m^3), **f)** Integrated Water Vapor (IWV, kg/m^2), **g)** Temperature (in °C) at 10 m above ground level, and **h)** ozone (O_3) mixing ratio (ppbv). Hg(0), IWV, and temperature were low from 5 to 20 February (period highlighted in red) while O_3 showed no abnormal variability.

Atmos. Chem. Phys. Discuss., doi:10.5194/acp-2016-144, 2016
Manuscript under review for journal Atmos. Chem. Phys.
Published: 18 February 2016

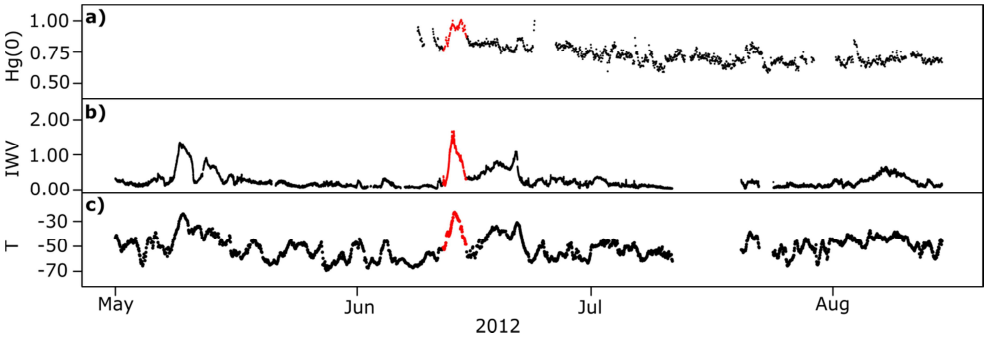

Figure 12: Year 2012 wintertime record of: **a)** hourly-averaged Hg(0) concentrations (in ng/m^3), **b)** Integrated Water Vapor (IWV, kg/m^2), and **c)** Temperature (T, °C) at 10 m above ground level. Hg(0), temperature, and IWV increased from June 12 to 15 (in red) suggesting transport of moist and warm air masses originating from lower latitudes